

Analysing Petroleum Leakage from Ground Penetrating Radar Signal



Zulkarnaini Mat Amin, Norwahidatul Akma Kamal,
Norhazimah Husna Shokri and Amalina Yusop

Abstract The current evolution of technologies and rapid development has influenced the pipeline construction all over the world. However, this development can be a risk to the surrounding environment, for example pipeline leakage. There are numerous incidents that caused by pipeline leakage, which includes petroleum pipeline leakage. The petroleum pipeline leakage is one of the very serious situations that can lead to the explosion and the worst it can cause disaster to the nearby area and loss of life. There are numerous methods that are used to detect underground pipeline leaks. One of the methods is Ground-Penetrating Radar (GPR). This study investigates the petroleum leakage and its impact to the surrounding soil. The objectives of this study are to determine the physical properties of the contaminated soil and to evaluate the numerical analysis of the electromagnetic wave for petroleum leakage diffusion in sand. The prototype of leakage model has been built for simulating observation. The data have been collected for every hour for 16 h to monitor the petroleum leakage diffusion. The software used to process and extract GPR data is Reflex 2DQuick. Furthermore, the Finite Difference Time Domain (FDTD) method was used for the simulation of the petroleum leakage diffusion by simulating the electromagnetic waves penetrating through different materials. GPR signal modelling and numerical analysis were done in MATGPR software. The result of this study indicates the changes of dielectric constant of sand from 3 to 5.3 when the sand is mixed with petroleum. The increase in dielectric properties of sand is due to its ability to store the electrical energy. Moreover, the result of GPR signal modelling proves that the content of petroleum has disturbed the signal attenuation which is transmitted by the antenna.

Z. M. Amin (✉) · N. A. Kamal · N. H. Shokri · A. Yusop
Geomatic Innovation Research Group, Faculty of Geoinformation
and Real Estate, Universiti Teknologi Malaysia, 81310 Skudai, Johor, Malaysia
e-mail: zulkarnaini@utm.my

© Springer Nature Singapore Pte Ltd. 2019
B. Pradhan (ed.), *GCEC 2017*, Lecture Notes in Civil Engineering 9,
https://doi.org/10.1007/978-981-10-8016-6_77

1087

1 Introduction

In the modern world, the infrastructure development is such a common thing. There are a lot of construction, excavation work and maintenance. All of this work needs a very high accuracy of geospatial data in order to avoid any mistake and serious problem during implementation. The pipeline leakage is one of the very serious situations that can lead to the explosion and the worst it can cause disaster to the nearby area and loss of life. The pipelines are used as a transportation medium of many resources such as water, gas, petroleum and others. The major reasons for pipeline leakage are erosion, mechanical failures, construction defeats, natural disaster and other reasons. There are numerous incidents caused by pipeline leakage all around the world especially the most dangerous pipeline which is petroleum pipeline leakage. It can lead to a very critical problem. Many cases of pipeline leakage are caused by excessive stress, corrosion and valve cracks and it starts from small cracks [1]. Other contributors to the pipeline leakage are natural disaster and construction works. One of the cases was reported on April 2014 in Malaysia. According to *The Star Online*, the incident occurred in Gua Musang, Kelantan caused 11 injured and 4 cars were burnt. There was an explosion caused by leaking hose when a tanker was filling up its underground tank. The leaking fuel flowed to the nearby food stall before catching fire [2].

Various methods are used to detect underground pipeline leaks and breaks. The common method that was used is acoustic devices [3], gas sampling devices, pressure wave detectors, microphone leak detection [4]. Each method has their own capabilities and weaknesses depending on the type and size of case area and the stage of the leakage occurred. One of the sophisticated methods is detection using Ground-Penetrating Radar (GPR). The word radar itself represented that this method used radio detection and ranging. It basically transmits the electromagnetic signals into the soil and the total time travelled of the emitted signals will be recorded [5]. GPR is a technology that is often used in various underground detections. It is a radar that generates an image based on the reflection of radar waves from soil, pipe or anything located underground. The advantage of using GPR for leak detection are it is known as a rapid measurement, noninvasive nature of the technique and its capability to detect defects before they reach an advanced phase. Unlike the other methods, application of GPR for leak detection is suitable for various type of pipe whether metal or non-metal. GPR is a higher potential method that can be used to avoid difficulties encountered with usually used acoustic leak detection [6]. Therefore, the underground detection by using GPR is the potential method that can be used for various cases. Besides, GPR serve as a non-destructive technique (NDT), which is very suitable for use in urban environments, as well as protecting the geological, environmental and archaeological [7].

As a rapid measurement technique, GPR directly gives a raw data after scans were done. The raw data must go through some processes of filtering before extracting the parameters. The interpretation and information from the GPR data

will be later used in numerical modelling known as Finite Difference Time Domain (FDTD) method. FDTD is one of the numerical modelling techniques, which implement the time domain method [8–10]. FDTD method is easy and simple, both conceptually and in terms of implementation, of the full-wave techniques is used to answer questions in electromagnetic problem [9].

In this study, data collection has been accomplished by using GPR. GPR can effectively locate metallic and non-metallic objects. However, it not suitable and cannot work in certain soil conditions, which contain high water such as clay. The penetration of GPR signal will be disturbed by the soil itself and thus the data obtained will be difficult to interpret. Soil is one of the elements of subsurface and it is defined as a top layer of the earth that also contains of mineral, water and decay organic. It can be considered as three phase mediums, which include soil matrix, air and water [11]. GPR signals are usually disturbed by water content in the soil. The detection ability of the objects and the contrast between dielectric value can be increased by the differences of water capacity in the background medium and the buried objects [12]. Soil properties parameters include the velocity and dielectric constant value. Each material has different value of velocity and dielectric constant. Even soil itself has different parameter based on different soil types.

2 Methodology

This study involved the design of special simulation tank to simulate the petroleum or specifically diesel leakage. The prototype laboratory model for this study which was shown in Fig. 1 was made up from fibreglass because of its less reflectivity, stability and strength. This prototype tank with a dimension of $2\text{ m} \times 2\text{ m} \times 2\text{ m}$ is filled with sand. A 1.8 m metal pipe was buried in this tank at 0.5 m depth. A hole was created at the middle of the pipe to simulate the pipe leakage situation. The

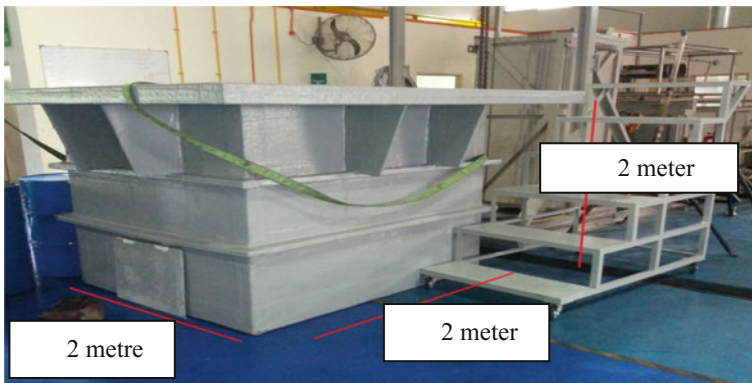


Fig. 1 Prototype laboratory tank

liquid flow into the pipe was controlled by the flow-line valve to monitor the volume of liquid pass into the simulation tank.

The equipment that was used in this study is GPR IDS Detector Duo. It is a multi-channel antenna with 250 and 700 MHz frequency, respectively.

2.1 Data Acquisition

Data collection for GPR survey was performed using grid method. Hence, grid lines were established at the top of the tank as shown in Fig. 2. Grid method consists of two scans which are longitudinal and transversal scan lines. Adoption of grid method for GPR survey is more systematic and as data was scanned along the designated lines at constant interval. Besides, a grid data can easily be used to create the three dimensional (3D) model.

2.2 Data Processing

Basic processing and filtering of GPR data were done using Reflex 2DQuick software [13]. In this study, the software was used to obtain the electromagnetic parameter of the contaminated soil and signal interpretation. The properties of contaminated soil by oil leakage are investigated by their physical behaviour. Therefore, the knowledge of soil properties is important in this study to differentiate the soil properties before and after contamination occurred. Further and advanced processing was executed using the MatGPR software [14]. The purpose of using this software is to create a FDTD simulation model and numerical analysis for this study.



Fig. 2 Top view of the tank and the grid system

The visual interpretation of the input data can be done in various options via inspecting traces, trace spectra and attenuation characteristics. In this study, the details of every data was investigated and analysed correctly in order to understand the flow of the leakage. Time–frequency analysis are done for each individual traces to compute a time frequency of that data. This time–frequency analysis is very useful in dispersion flow and propagation characteristic. In this case, the focus of time–frequency analysis is only for longitudinal data because it shows the clear visualization of the dispersion compared to the transversal data. Other than that, data can also be analysed using attenuation characteristics. This attenuation analysis is used to determine the mean and median attenuation of all traces. Based on the attenuation analysis, it can obtain the best-fitting exponential decay curve and the best-fitting power-law decay curve.

3 Results and Analysis

3.1 Data Interpretation

GPR provides data in the form of radargram based on the signal propagation and properties of underground materials. The IDS Detector Duo GPR instrument used dual frequencies in data collection. In this study, the higher frequency was used focus to provide better resolution for 2 metres depth. The benefit of high frequency is it provides a good resolution data for data interpretation. Figure 3 shows the radargram of the observation data at 1 and 10 h. The change of the reflected signal can be seen in the radargram due to the existence of different materials from the soil. The reflection represents the content of the petroleum in the sand. The differences of the reflected signals, where the petroleum spill occurred can be seen in each radargram.

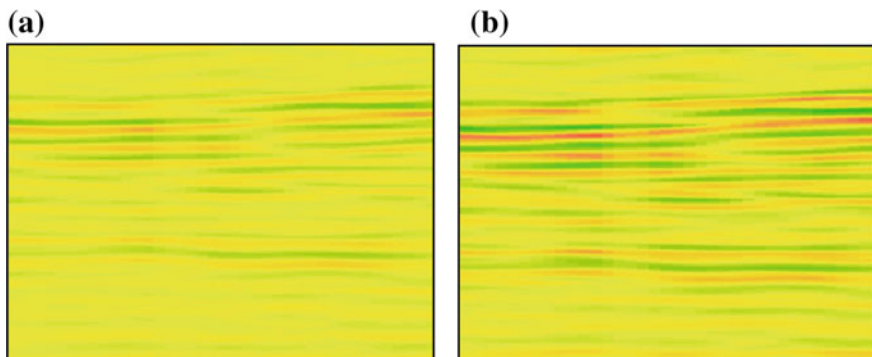


Fig. 3 Radargram of the petroleum leakage at 1 h (a) and 10 h (b)

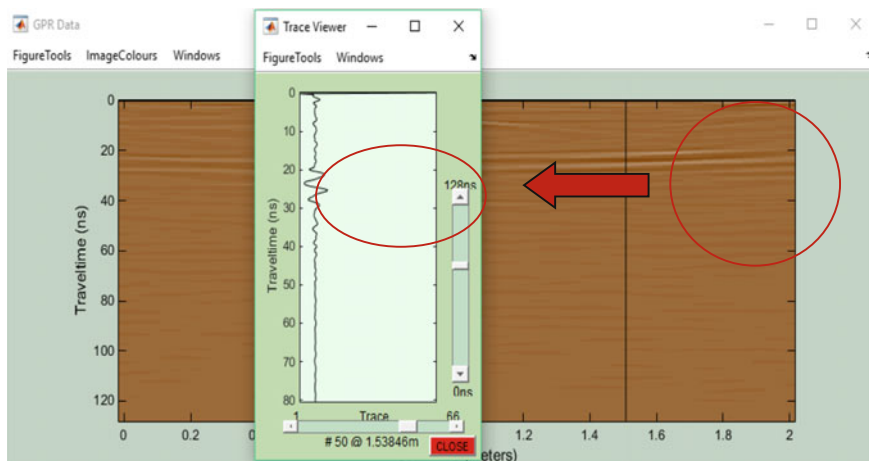


Fig. 4 Trace viewer at trace 50

The leakage occurrence has interrupted the propagation of the GPR signal. Therefore, the signal propagation at the spill area was analysed using trace viewer as marked in Fig. 4. The signal was disturbed at travel time 20–30 ns (see red circle), which are around 1.2–1.9 m depth.

3.2 Parameters Extraction from GPR Data

GPR transmits the electromagnetic signal into the ground and the signal will be reflected back to the antenna as it touches any underground material. Therefore, the time travel recorded from the signal can be used to define the depth and location of the object. Penetration of signal depth is influenced by the antenna frequency that has been used in data collection. The higher the antenna frequency, the shorter the signal penetration. All materials have their own dielectric constant value depending on the ability to store the electrical energy. The normal dielectric constant for sand is 3 and the value of the dielectric constant obtained after sand mixed with petroleum have changed. Table 1 shows the value of dielectric constant that is calculated from the observation data using Eq. 1. The dielectric constant is calculated for

Table 1 Parameters of the contaminated sand obtained from the radargram

Time (h)	Velocity (m/ns)	Soil dielectric constant
1	0.1702	3.1
4	0.1538	3.8
8	0.1499	4.0
12	0.1398	4.6
16	0.1302	5.3

every 4 h observation. Results show the value of dielectric increase as the observation hours increase. It can be concluded that dielectric constant of uncontaminated sand and contaminated sand are different and about 2.3 dielectric constant increase from its original value. The value of velocity is inversely proportional to the dielectric constant which is decreases as the dielectric constant increases.

$$v = \frac{c}{\sqrt{\epsilon}} \tag{1}$$

where

- v is the electromagnetic signal velocity
- c is the speed of light in vacuum
- ϵ is the dielectric constant of the material.

3.3 Signal Modelling

2D Model of the prototype tank was created in order to be used in the FDTD simulation. The properties of the 2D model that has been created follow exactly the real prototype with depth and distance 2 m each. Metal pipe was illustrated at the 0.5 m depth (Fig. 5).

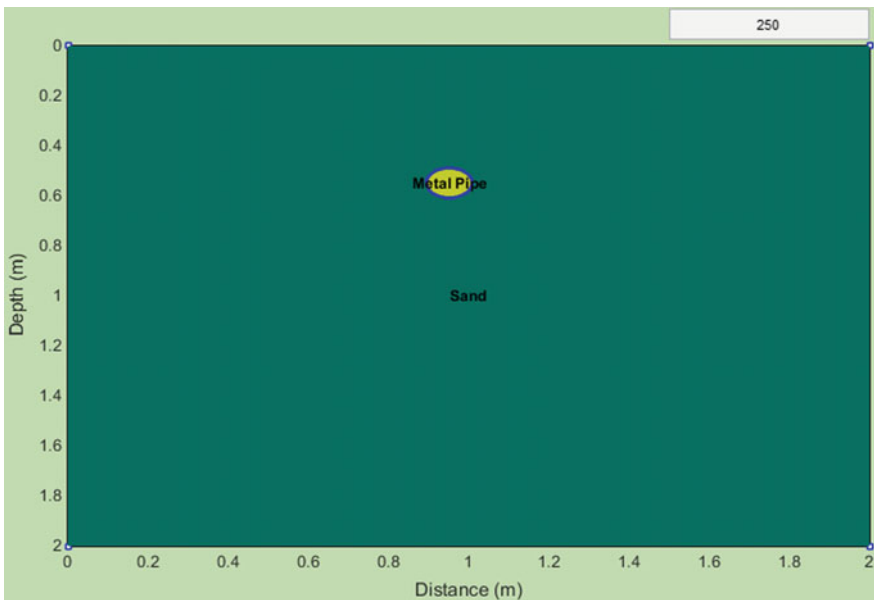


Fig. 5 2D model of the tank

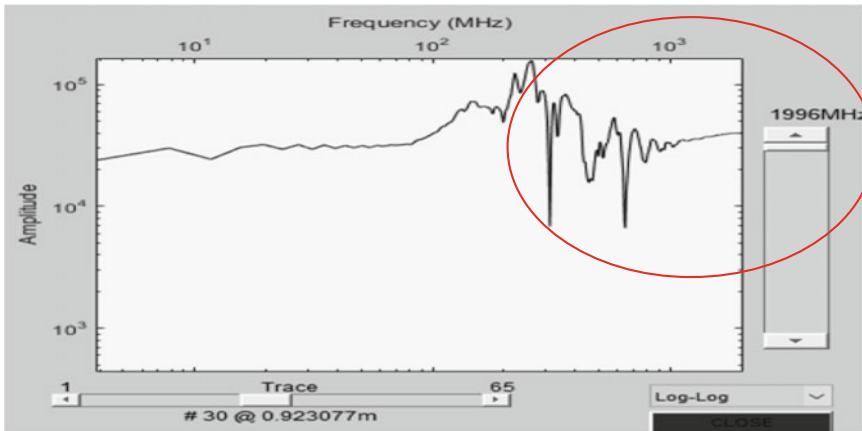


Fig. 6 Amplitude of the metal pipe at trace 30

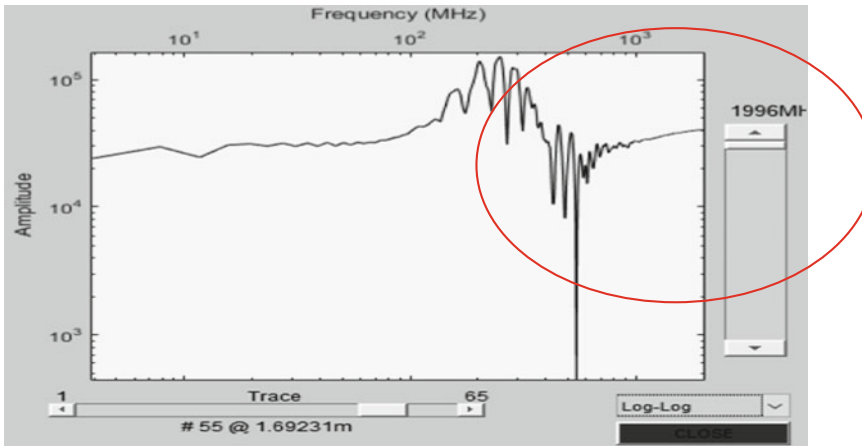


Fig. 7 Amplitude of the pipe leakage at trace 55

Figure 6 shows the amplitude of the signal fluctuation due to the metal pipe. This pipe which has a dielectric constant of 14 mostly impacts the amplitude. Conversely Fig. 7 shows the impact of petroleum in sand. As illustrated in the amplitude graph, the average of the fluctuated peak is varied. This is because the particles of petroleum and the sand was not completely mix together.

3.4 Analysing Electromagnetic Properties Between Contaminated and Uncontaminated Soil

The dielectric constant value represents the capability of a material to hold the electrical energy. Contaminated sand with petroleum has different dielectric constants because its structural and electromagnetic properties have been disturbed. Figure 8 shows the graph comparison between normal and contaminated value of sand dielectric constant. It can be seen in the graph that the dielectric value of contaminated sand increases with hour. At the end of observation, the dielectric constant goes up until 5.3 which is different from the normal value 2.3. The straight line represents dielectric constant for normal dry sand, while star symbol represents the dielectric constant for contaminated sand. Sample number 1 in x -axis is observed in the first hour of leakage, samples number 2, 3, 4 are observed at hour 4, 8, 12 after leakage occurred and sample number 5 was taken at the last hour of observation.

Conversely, the graph in Fig. 9 illustrated the differences in the relationship of velocity and observation time, dry and contaminated sand with petroleum. Straight line graph with a of value 0.17 m/ns represented the normal velocity in sand with dielectric constant 3. As can be seen in the figure, the graph continuously declines until sample 5 which is hour 16 of observation. The petroleum leakage flow increases for each hour which means the volume of the petroleum mixed with sand increased. Therefore, the higher volume of petroleum mixed with sand, the lower the velocity value.

3.5 Attenuation Characteristics Analysis

GPR collected underground data by transmitted electromagnetic wave into the ground. Every signal transmitted is differentiated by its trace number. The

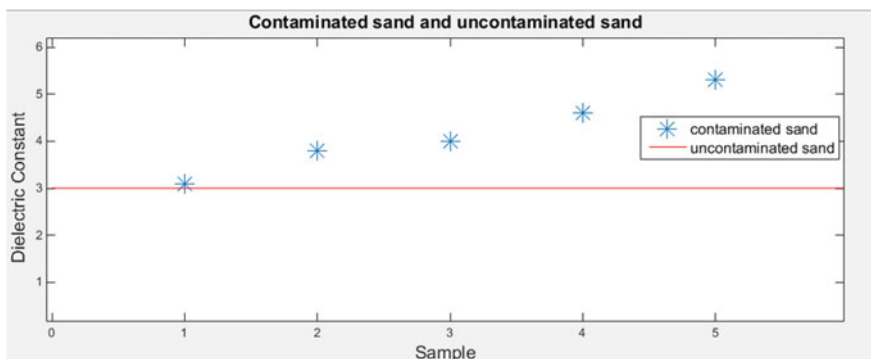


Fig. 8 The graph of comparison of dielectric constant between contaminated sand with petroleum and the normal value of dielectric constant

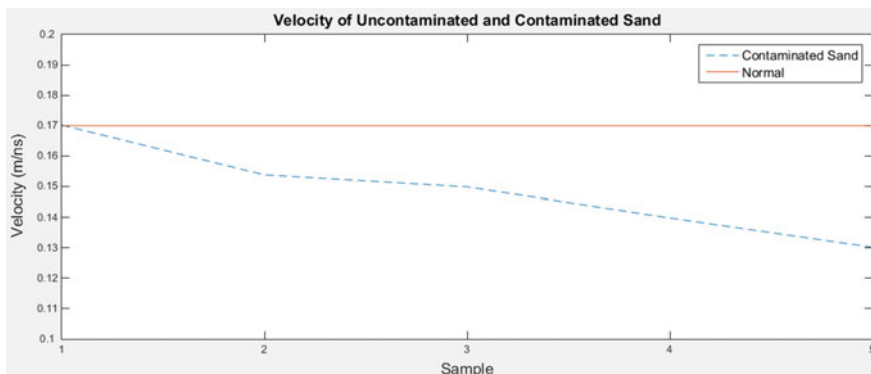


Fig. 9 The graph of comparison velocity between the signal in contaminated sand with petroleum and the uncontaminated sand

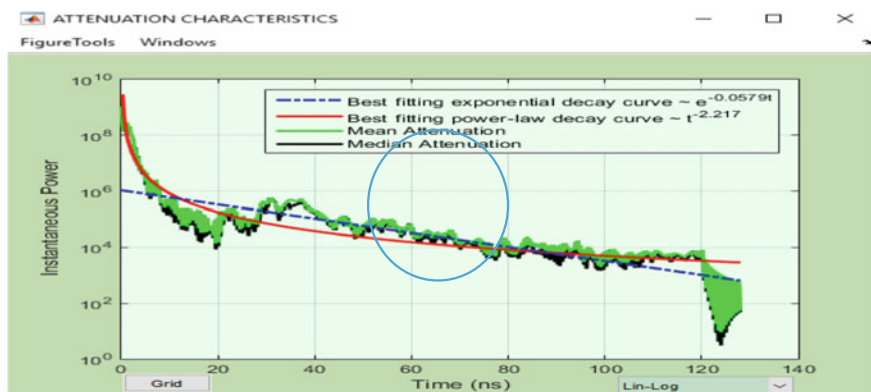


Fig. 10 Attenuation graph of instantaneous power against time (ns) at 1 h

attenuation of the electromagnetic signal is one of the important elements while investigating the flow of the petroleum leakage, since it will be used to obtain the optimal gain function. Figures 10, 11, 12 and 13 illustrate the attenuation characteristics graph of the GPR signal. As the signal goes further which increases in time, the power of the signal is decreased gradually. The mean and median attenuation at time around 20–30 ns are increased and slightly fluctuate due to signal interference. The interference is assumed to be occurring because of the leakage since the radargram of the observation data shows the reflection of the leakage are around time 20–30 ns. The differences of the attenuation between the observation data can be seen in those figures. The graph for signal fitting is also illustrated. The fitting model includes exponential decay and power-law decay. The process of fitting

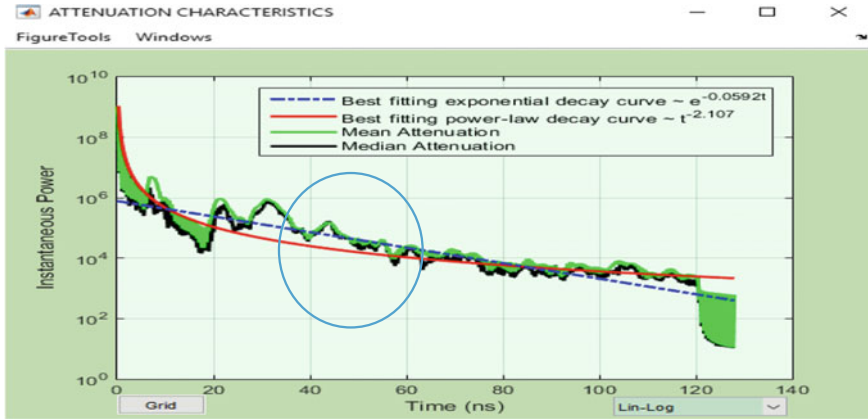


Fig. 11 Attenuation graph of instantaneous power against time (ns) at 5 h

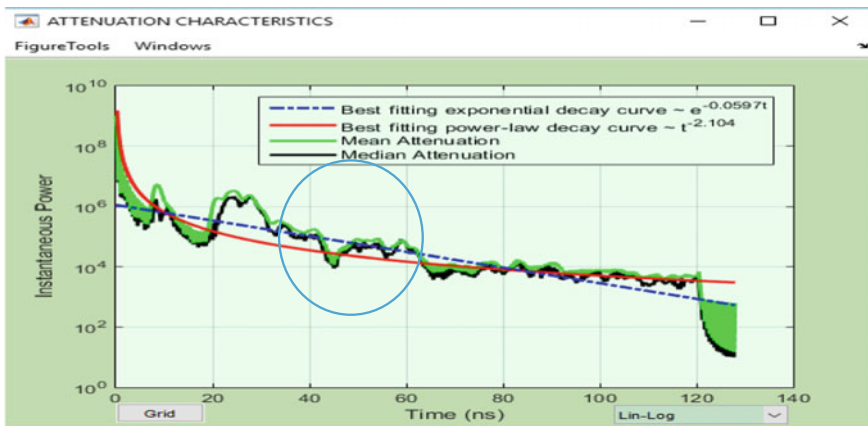


Fig. 12 Attenuation graph of instantaneous power against time (ns) at 10 h

exponential decay is one of the modelling data using exponential function. The best-fitting exponential decay curve at $e^{-0.0579t}$ of attenuation power is decrease with time travel of the signal as can be seen at 1 h observation data. Meanwhile, the best-fitting power-law decay curve at $t^{-2.217}$ drastically falls from time 0 to 20 ns, then it decrease slowly along the time.

The value of attenuation power at the last observation hour is higher compared to the hour before. As can be seen the highest peak of the attenuation at 1 h data is below 10^6 . Then it increases along the observation time and the highest peak of the attenuation at 16 h is more than 10^6 .

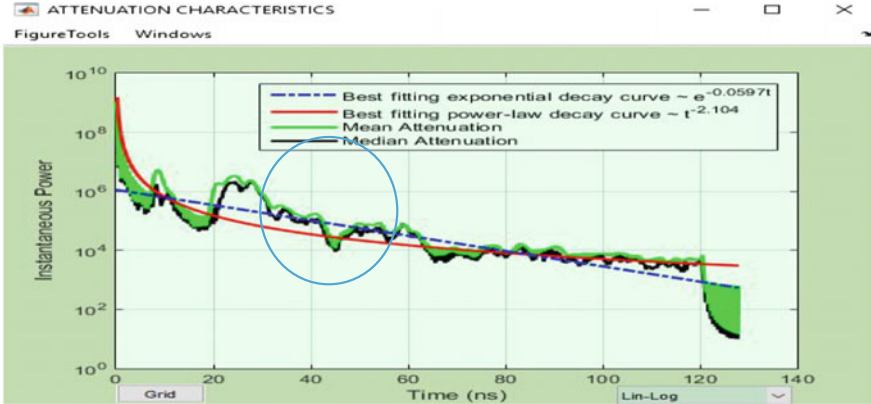


Fig. 13 Attenuation graph of instantaneous power against time (ns) at 16 h

3.6 Interpretation of Radargram Obtained from Simulation and GPR Survey

This study produces the theoretical prediction by implementing FDTD simulation. The comparison between results obtained from the simulation and the radargram can be used to enhance data interpretation, reduce the errors and even predict the reflection of the underground medium and materials. Radargram in Fig. 14 was obtained from the observation data carried out in this study using 250 MHz frequency. The parabola shape from the reflected signal of metal pipe can be seen clearly in the radargram. The 1 m metal pipe was buried at 0.5 m from the surface. The 2D model in Fig. 15 was created using MATGPR Model Builder. The metal pipe was placed exactly like the real prototype set up. The frequency which has

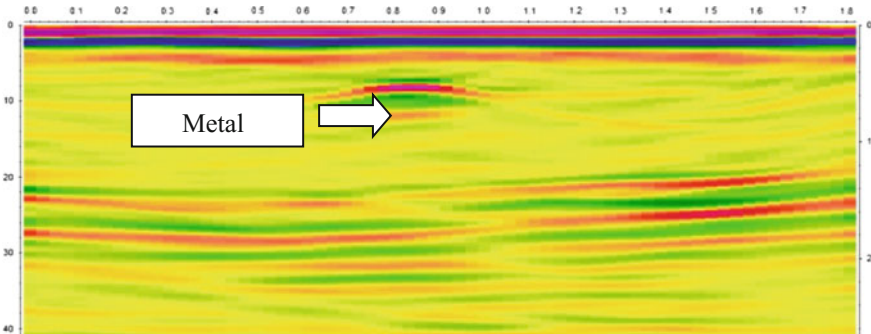


Fig. 14 Radargram data obtained from observation

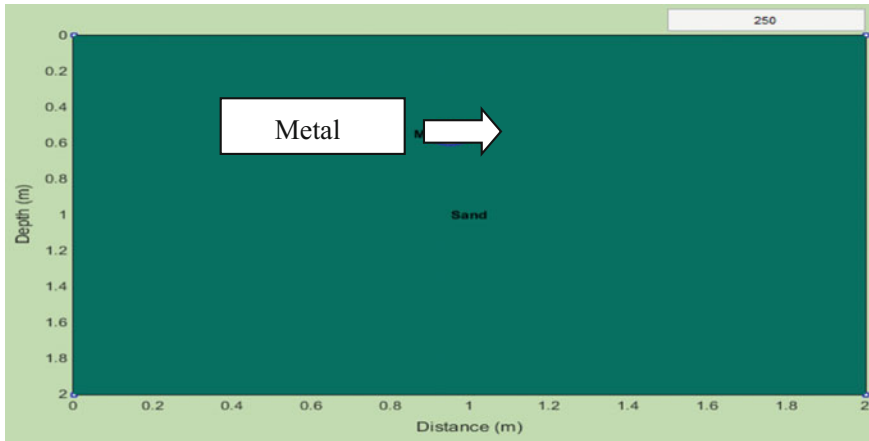


Fig. 15 2D model of the tank

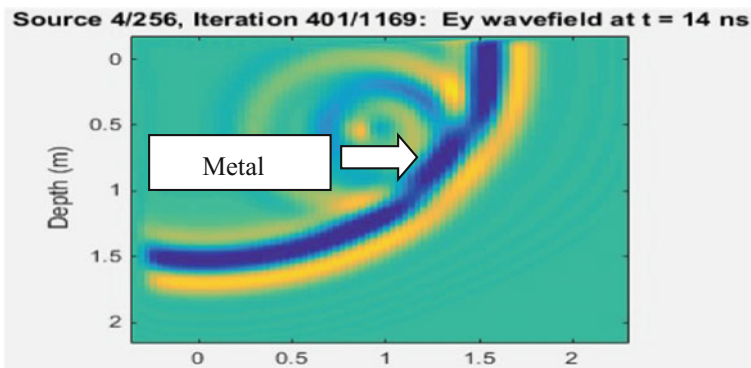


Fig. 16 FDTD simulation

been set for the whole model is 250 MHz and every detail object or medium in the model are created using their own electromagnetic properties. Dielectric value of metal pipe is 14 while sand is 3. FDTD simulation as shown in Fig. 16 is an animation of iteration process. The synthetic model was obtained from the FDTD simulation as the prediction of the scanned data. Therefore, the synthetic model must be identical with response from the radargram. The position of the metal pipe parabola is similar with the radargram with time travel of 10 ns. A noticeable dissimilarity between radargram and synthetic model is the presence of the other reflection due to the petroleum leakage flow (Fig. 17).

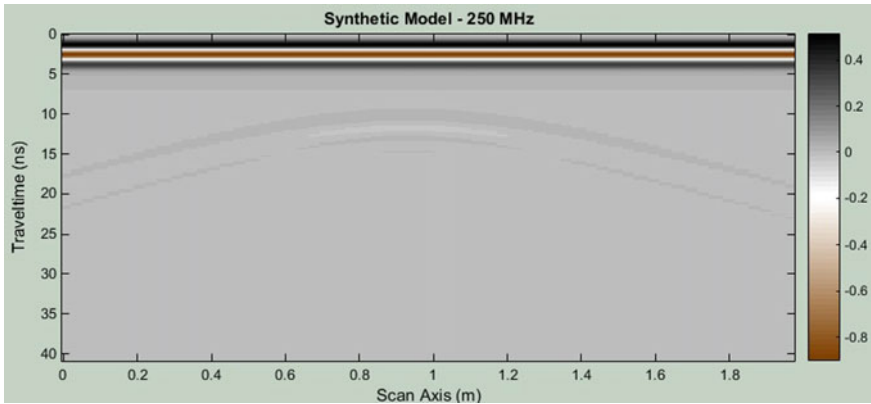


Fig. 17 Synthetic model obtained from FDTD Simulation of 2D model

4 Conclusion

Electrical properties of the soil influenced the applications of GPR. The interpretation of the GPR data requires the knowledge of the soil properties, electromagnetic characteristic of the materials in order to produce high-quality results as accurate as possible. Furthermore, the underground detection must be done accurately to avoid any hazardous in further works. Therefore, one of the objectives in this study is to determine the physical properties of the contaminated soil with petroleum. Even though, crude oil such as petroleum has less dielectric constant value and electrical conductivity than water, it still gives an impact to the electromagnetic signal. Consequently, GPR technique is capable to be used in detection flow of the petroleum leakage. Through this study, the physical changes of the soil properties when mixed with petroleum have been identified. Besides, the attenuation analysis also has been done for each data since it affects the propagation of the wave through a medium. Attenuation is directly proportional to the electrical conductivity. Therefore, the materials with high electrical conductivity will create high attenuation. In this study, the simulation was implemented to predict the flow of system and petroleum leakage. The simulation is a necessary step in some cases which could not implement the physical test due to the risk, cost and time consuming. The synthetic model obtained from the simulation has illustrated the same image as shown in observation data. The simulation result was compared with the radargram to improve the data interpretation and minimize errors. In addition, the numerical analysis was done to analyse the signal propagation and properties. The conclusion can be made from this study is GPR survey and basic filtering processes can be done by anyone but an experienced and knowledgeable operator for advance interpretation is required. The advance interpretations mentioned are the signal interpretation and modelling has been done in this study. Nevertheless,

further study can be pursued by applying real pressure equipment or system to create the real rate flow of the liquid and comparison of the pipe leakage detection in different types of soils.

Acknowledgements The authors gratefully acknowledge the Ministry of Higher Education, Malaysia and Universiti Teknologi Malaysia for their kind financial support through FRGS research grant (R.J130000.7827.4F467).

References

1. Lilly, M.T., Ihekwoaba, S.C., Ogaji, S.O.T., Probert, S.D.: Prolonging the lives of buried crude-oil and natural-gas pipelines by cathodic protection. *Appl. Energy* **84**(9), 958–970 (2007)
2. Syed Azhar, C.A.Z.: 11 hurt in blaze at R&R stop. *The Star Online*. April 2014
3. Xu, Q., Zhang, L., Liang, W.: Acoustic detection technology for gas pipeline leakage. *Process Saf. Environ.* **91**(4), 253–261 (2013)
4. Shimanskiy, S., Iijima, T., Naoi, Y.: Development of microphone leak detection technology in Fugen Nuclear Power Plant. *Saikuru Kiko Giho*, 67–77 (2002)
5. Rebecca Ludwig, H.G., Klenk, P., Wollschlager, U., Buchner, J.: *Electromagnetic Methods in Applied Geophysics* (2011)
6. Hunaidi, O., Giamou, P. (eds.): Ground-penetrating radar for detection of leaks in buried plastic water distribution pipes. In: *International Conference on Ground Penetrating Radar* (1998)
7. Gamba, P., Lossani, S.: Neural detection of pipe signatures in ground penetrating radar images. *IEEE Trans. Geosci. Remote Sens.* **38**(2), 790–797 (2000)
8. Yee, K.S., Chen, J.S.: Impedance boundary condition simulation in the FDTD/FVTD hybrid. *IEEE Trans. Antennas Propag.* **45**(6), 921–925 (1997)
9. Schneider, J.B.: *Understanding the Finite-Difference Time-Domain Method* (2017)
10. Connor, S.: Introduction to the finite-difference time-domain (FDTD) technique. In: *2008 IEEE International Symposium on Electromagnetic Compatibility*, vols. 1–3, 972–981 (2008)
11. Rebecca Ludwig, H.G., Klenk, P., Wollschlager, U., Buchner, J.: *Electromagnetic Methods in Applied Geophysics*, p. 64. CreateSpace Independent Publishing Platform (2014)
12. Lauro, S.E., Mattei, E., Barone, P.M., Pettinelli, E., Vannaroni, G., Valerio, G., et al.: Estimation of subsurface dielectric target depth for GPR planetary exploration: laboratory measurements and modeling. *J. Appl. Geophys.* **93**, 93–100 (2013)
13. Sandmeier, K.J.: *ReflexW 7.2 Manual Book*. Karlsruhe, Germany (2013)
14. Tzanis, A.: *MATGPR, Manual and Technical Reference*. Department of Geophysics UoA, editor (2013)